Human Molecular Genetics, 2017, Vol. 26, No. 9 1694–1705

doi: 10.1093/hmg/ddx075
Advance Access Publication Date: 1 March 2017
Original Article

ORIGINAL ARTICLE

The Wilms tumor protein Wt1 contributes to female fertility by regulating oviductal proteostasis

Abinaya Nathan[1], Peter Reinhardt[1,†], Dagmar Kruspe[1], Tjard Jörß[2], Marco Groth[3], Hendrik Nolte[4,‡], Andreas Habenicht[5,¶], Jörg Herrmann[6], Verena Holschbach[7,#], Bettina Toth[7], Marcus Krüger[4,‡], Zhao-Qi Wang[2], Matthias Platzer[3] and Christoph Englert[1,8,*]

[1]Molecular Genetics Lab, [2]Genomic Stability Lab, [3]Genome Analysis Lab, Leibniz Institute on Aging – Fritz Lipmann Institute (FLI), Jena, Germany, [4]Max Planck Institute for Heart and Lung Research, 61231 Bad Nauheim, Germany, [5]Institute for Vascular Medicine, Jena University Hospital, Jena, Germany, [6]Department of Gynecology and Obstetrics, Hufeland Klinikum, 99425 Weimar, Germany, [7]Department of Gynecological Endocrinology and Fertility Disorders, University Hospital Heidelberg, 69120 Heidelberg, Germany and [8]Institute of Biochemistry and Biophysics, Friedrich-Schiller-University Jena, 07745 Jena, Germany

*To whom correspondence should be addressed at: Leibniz Institute on Aging - Fritz Lipmann Institute (FLI), Beutenbergstr. 11, 07745 Jena, Germany. Tel: +49 3641656042; Fax: +49 364165695335; Email: christoph.englert@leibniz-fli.de

Abstract

Although the zinc finger transcription factor Wt1 has been linked to female fertility, its precise role in this process has not yet been understood. We have sequenced the *WT1* exons in a panel of patients with idiopathic infertility and have identified a missense mutation in *WT1* in one patient out of eight. This mutation leads to an amino acid change within the zinc finger domain and results in reduced DNA binding. We utilized $Wt1^{+/-}$ mice as a model to mechanistically pinpoint the consequences of reduced Wt1 levels for female fertility. Our results indicate that subfertility in $Wt1^{+/-}$ female mice is a maternal effect caused by the Wt1-dependent de-regulation of *Prss29*, encoding a serine protease. Notably, blocking Prss29 activity was sufficient to rescue subfertility in $Wt1^{+/-}$ mice indicating Prss29 as a critical factor in female fertility. Molecularly, Wt1 represses expression of *Prss29*. De-repression and precocious expression of *Prss29* in the oviduct of $Wt1^{+/-}$ mice interferes with pre-implantation development. Our study reveals a novel role for Wt1 in early mammalian development and identifies proteases as critical mediators of the maternal-embryonic interaction. Our data also suggest that the role of Wt1 in regulating fertility is conserved in mammals.

[†]Present address: Neuroscience Discovery, Biology Department, AbbVie Deutschland GmbH & Co. KG, Ludwigshafen, Germany.
[‡]Present address: Institute for Genetics and CECAD, University of Cologne, 50931 Cologne, Germany.
[¶]Present address: Institute for Cardiovascular Disease Prevention, Ludwig Maximilians University (LMU) Munich, Pettenkoferstr. 9, 80336 Munich, Germany.
[#]Department of Gynecological Endocrinology and Reproductive Medicine, Medical University Innsbruck, Anichstrasse 35, 6020 Innsbruck, Austria.
Received: December 16, 2016. **Revised:** February 22, 2017. **Accepted:** February 23, 2017

Introduction

Despite progress in research on female infertility and improvement in assisted reproductive technologies, at least 20% of cases remains undefined, referred to as idiopathic female infertility (1). *Wt1*, originally identified as a Wilms tumor suppressor gene, is required for the development and homeostasis of several organs including the heart, kidney, oviduct, ovary and the testes (2–5). In mice, *Wt1* heterozygosity has been correlated with strain-dependent subfertility due to a function for Wt1 during preimplantation embryonic development (6). However, the molecular mechanisms underlying this phenotype manifestation remain to be elucidated.

Ovulated oocytes travel towards the infundibulum of the oviduct where fertilization occurs. The highly ciliated epithelial cells in the infundibulum of the oviduct assist in the funneling of the oocyte-cumulus complexes toward the ampulla, where the sperm penetrates the oocyte-cumulus complex and enters the peri-vitelline space (7). Upon fertilization, the cumulus cells are lost and the now zygote, undergoes blastomere cleavage whilst travelling through the oviduct (7). At embryonic day 4.5 (E4.5) the mature blastocyst proceeds to the uterus, ready for implantation. Embryo development in the oviduct is a highly orchestrated process, regulated by several components to define the maternal-embryo interface.

The infundibulum and ampulla consist mainly of ciliated epithelial cells whereas the distal part of the oviduct, the isthmus and the uterotubal junction, consist largely of secretory 'peg' cells. The 'peg' cells contain apical granules and secrete factors required for gamete survival, fertilization and embryo development. The composition of the oviductal fluid has been identified to be growth factors, cytokines, hormones, proteases and inhibitors, glycosidases, and heat shock proteins, by comparative studies in the oviductal fluid of human, mice, rat and rabbit (8). It has been suggested that the epithelial cells act as 'gate- keepers' of the nutrients present in the oviductal fluid, thereby emphasizing the long-term impact of the fluid composition on the developing embryo (9).

Here, we ask whether WT1 plays a role in human female fertility by performing exome sequencing of the WT1 locus in patients with idiopathic infertility. The identification of a missense mutation in a patient led us to explore how Wt1 is required to maintain female fertility by orchestrating preimplantation embryonic development in the mouse oviduct. By analyzing fertility in $Wt1^{+/-}$ mice, transcriptional profiling of the oviductal cells, along with proteomic analysis of the oviductal fluid composition, we show that *Wt1* maintains female fertility by repressing oviductal expression of *Prss29*, encoding a protease that is active in the uterus.

Results

A loss-of-function WT1 mutation in a patient suffering from infertility

Recently, a novel *WT1* missense mutation, R370H, was identified to be a factor involved in premature ovarian failure (10). This was shown to be due to WT1's role in granulosa cell differentiation, similar to Wt1(+/R394W) mice where infertility was due to aberrant ovarian follicle development (11). On the contrary, subfertility in $Wt1^{+/-}$ mice is not due to a problem in granulosa cell differentiation (6).

In order to examine whether in humans WT1 might also be involved in cases of reduced fertility that is not caused by the ovary, we asked whether *WT1* was expressed in the human oviduct. By analysing three independent samples of human fallopian tubes, we found that WT1 localized to nuclei of epithelial cells lining the oviduct (Fig. 1A and Supplementary Material, Fig. S1A), a result that was confirmed by immunoblot analysis (Supplementary Material, Fig. S1B). Next, we screened eight patients below 40 years of age diagnosed with unexplained female infertility for *WT1* mutations. Upon sequencing all ten exons of *WT1*, we have identified one heterozygous single nucleotide variation in exon 7 (1238G > T) in one patient. This SNV results in a missense mutation within zinc finger one of WT1 (R413M; NP_077744.3) (Fig. 1B). This exact *WT1* mutation has been found once, thus far, in the Exome Aggregation Consortium database (rs373176048) involving 60,706 individuals, resulting in an allele frequency of 0.000008240. Three other patients showed variations in exon 1, 7 and intron 2 of *WT1* that did not affect their amino acid sequence (Supplementary Material, Table S1). Since the arginine at position 413 within the DNA binding domain is highly conserved among several zinc finger transcription factors (Supplementary Material, Fig. S1C), we aimed to determine whether the R413M mutation in WT1 affected its DNA binding capability. WT1 has been shown to bind to a sequence also recognized by the Early Growth Response-1 (EGR-1) protein (12). Consistent with previous data, we observe that wild type WT1 protein bound to the EGR1 consensus sequence (Fig. 1C), however, the same sequence was not bound by mutant WT1 (Fig. 1C, Supplementary Material, Fig. S1D). Thus, the *WT1* mutation that we have detected in an infertile patient results in a WT1 protein with reduced DNA binding activity.

Subfertility of $Wt1^{+/-}$ mice is mediated by the oviduct

Consistent with observations by others (6), we noted reduced fertility of *Wt1* heterozygous female mice in backgrounds other than B6, such as in MF1 and 129/Sv (Supplementary Material, Fig. S2A). To determine the earliest stage at which embryo development was disrupted, we analysed the number of embryos obtained from *Wt1* heterozygous MF1 mothers at different time points during pregnancy. We observed that the number of preimplantation stage embryos in $Wt1^{+/-}$ females was reduced from as early as E2.5 (embryonic day 2.5) (Fig. 2A). Since *Wt1* is known to be expressed in the granulosa cells of primary follicles in the ovary (11,13), we asked whether folliculogenesis was affected. When quantifying the number of *corpora lutea*, the remnant of a follicle following ovulation which indicates oocyte maturation (14), we observed no difference between genotypes from E2.5 to E11.5 (Supplementary Material, Fig. S2B). This finding, along with the comparable number of oocytes produced by wild type and $Wt1^{+/-}$ mice (Supplementary Material, Fig. S2C) demonstrated that the oocyte maturation and stimulation was not significantly affected in $Wt1^{+/-}$ mice.

To explain the cause of this subfertility, we transferred wild type embryos at E1.5 to both wild type and $Wt1^{+/-}$ pseudopregnant females. Analysing the number of embryos at E3.5, we observed that fewer embryos could be retrieved from $Wt1^{+/-}$ females than that from wild type hosts (Fig. 2B). It was apparent that, at E3.5, significantly fewer blastocysts could be obtained from $Wt1^{+/-}$ mice (Supplementary Material, Fig. S3A and B). Consistent with expression in the human oviduct, *Wt1* is expressed in the epithelial cells lining the oviduct (Fig. 2C). Notably, *Wt1* is expressed in a gradient fashion in the oviduct; strongest proximally (towards the ovary) and gradually becoming weaker distally (towards the uterus) (Fig. 2D, Supplementary

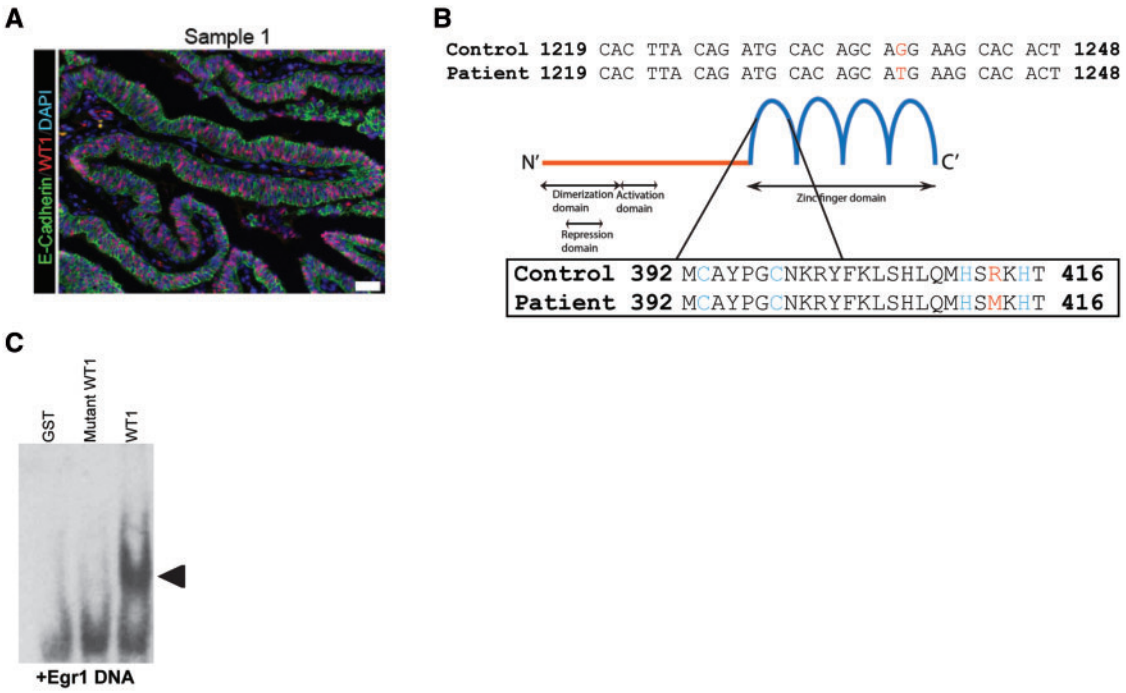

Figure 1. WT1 variant from an infertile patient shows reduced DNA binding capability. (**A**) Image of immuno-staining of a human fallopian tube sample depicting WT1 (red) overlapping with E-cadherin (green). Scale bar, 20 μm; DAPI, 4',6-diamidino-2-phenylindole. (**B**) Single nucleotide variation (SNV) found in a patient with idiopathic infertility within exon 7 of the *WT1* locus (1238G>T). The SNV results in a missense variation (R413M; NP_077744.3). Exon 7 of *WT1* codes for the first zinc finger. (**C**) Gel shift assay using wild type and mutant Wt1 and the *Egr1* DNA consensus sequence. GST alone served as a control. The arrowhead marks the band representing DNA bound by Wt1.

Material, Fig. S4A). The expression of *Wt1* was reduced in oviducts of $Wt1^{+/-}$ mice (Supplementary Material, Fig. S4B).

To assess the role of Wt1 in maternal - embryo communication, we established primary oviduct cells (pOCs) by employing a $Wt1^{fl/fl}$; $Rosa26\text{-}Cre^{ERT2}$ (*Wt1cKO*) mouse line, which deletes *Wt1* *ex vivo* upon 4'-hydroxytamoxifen administration. By culturing wild type E1.5 embryos in the presence of pOCs, we observed that cleavage rates of embryos grown on *Wt1*-deleted pOCs were inferior to that of embryos cultured on wild type pOCs (Fig. 2E). Fewer embryos grown on *Wt1cKO* pOCs reached the morula (at day 2) and blastocyst stages (at day 3), providing evidence that loss of *Wt1* in oviductal cells has a negative effect on embryo development (Supplementary Material, Fig. S5A).

Based on our observations, we hypothesized that the short exposure of embryos to a milieu with reduced Wt1 impeded embryo development. To test this idea, we transferred embryos that had, until E1.5, been habituated to the oviductal microenvironment in $Wt1^{+/-}$mice, to pseudopregnant wild type mothers. We retrieved embryos at E3.5 and found that embryos that had been transferred from $Wt1^{+/-}$ animals were less developed compared to embryos transferred from wild type mothers. A result that became evident after analyzing the number of morulae and blastocysts (Supplementary Material, Fig. S5B) as well as the total number of embryos recovered (Fig. 2F). This data suggest an irreversible effect on the embryos conferred by the $Wt1^{+/-}$oviductal environment.

Levels of oviductal proteases and protease inhibitors are altered in $Wt1^{+/-}$ mice

The oviductal fluid contains factors secreted by the epithelial cells and provides a microenvironment suitable for early embryo development (15). To study Wt1-dependent molecular alterations that might affect maternal fertility, we analyzed the oviductal fluids of $Wt1^{+/+}$and $Wt1^{+/-}$ mice. By performing quantitative mass spectrometry (LC-MS) comparing the oviductal fluid proteome of $Wt1^{+/+}$and $Wt1^{+/-}$ mice at E2.5, we found 37 significantly altered proteins (p value < 0.05 and fold change > 2) (Fig. 2G, Supplementary Material, Table S2). In the fraction of altered extracellular proteins, we found a trypsin-like serine protease encoded by the gene *Prss29*, which is required in the uterus for blastocyst hatching and implantation (16–18), with >30 fold increased expression in $Wt1^{+/-}$ mice compared to $Wt1^{+/+}$mice. Conversely, the relative increase in *Prss29* expression was accompanied by a significant decrease in three serine protease inhibitor proteins (Itih1, Itih2 and Serping1) in the oviduct of $Wt1^{+/-}$ mice. Similarly, *Prss29* was also upregulated in $Wt1^{+/-}$ mice in whole oviductal RNA as shown by our microarray (MA) data (Supplementary Material, Fig. S6A). This was further confirmed by qPCR on RNA from oviducts and pOCs (Supplementary Material, Fig. S6B and C) as well as immunoblotting using oviductal fluid (Supplementary Material, Fig. S6D). Furthermore, we investigated the spatial localization of Prss29 in the oviduct using immunohistochemical staining which revealed its localization to the epithelial cells of the oviduct restricted to $Wt1^{+/-}$ mice (Fig. 2H). Prss29 was not detectable in the oviducts from wild type mice. Consistent with our observations that fertility was not affected in $Wt1^{+/-}$ female B6 mice, we observed that Prss29 could not be detected in epithelial cells of the $Wt1^{+/-}$ (B6) oviducts, as in $Wt1^{+/-}$ (129/Sv) and (MF1) oviducts (Supplementary Material, Fig. S6E).

Wt1 represses *Prss29* expression

These observations prompted us to investigate the binding of Wt1, as a potential transcriptional repressor, to the *Prss29* gene.

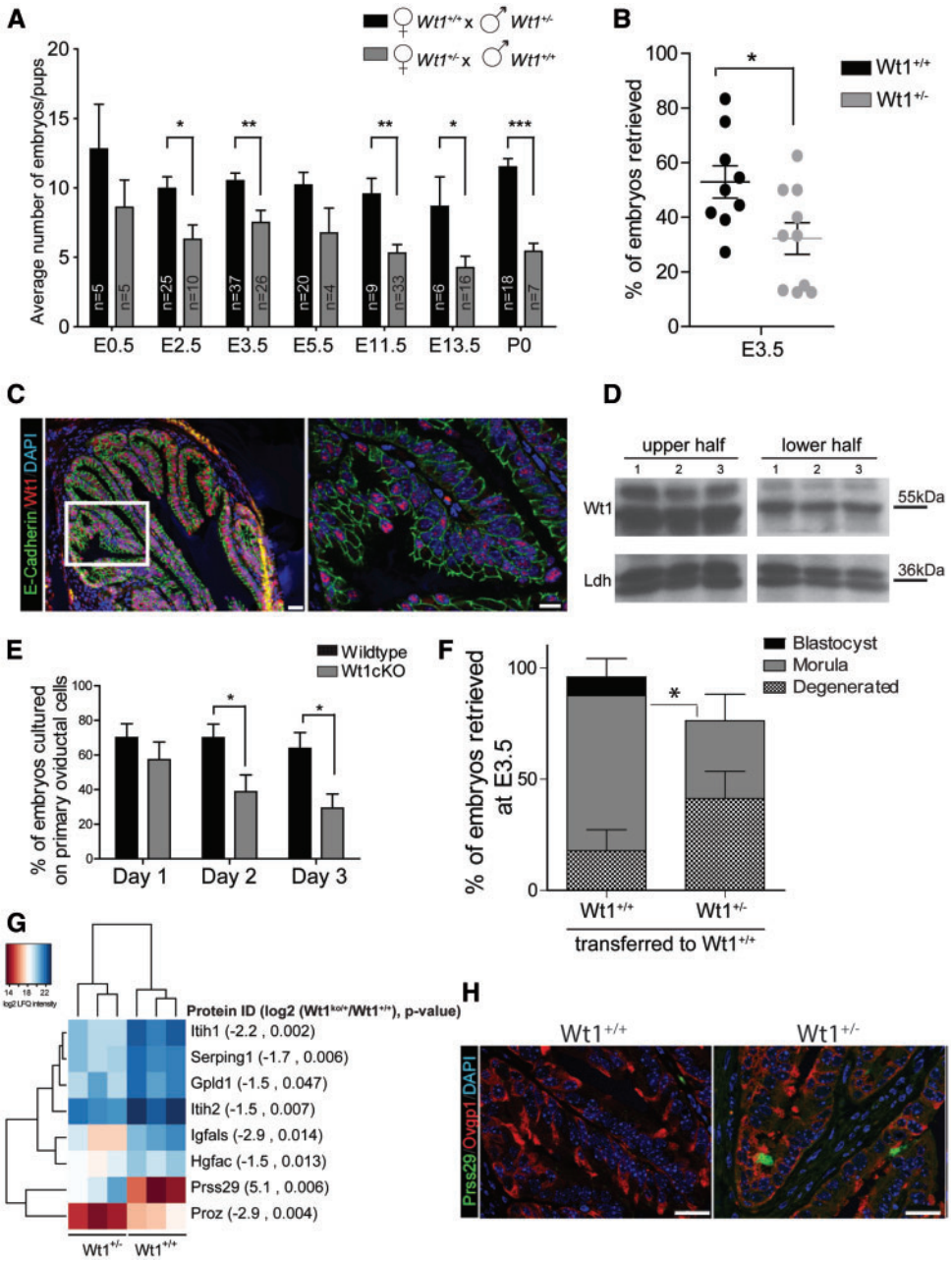

Figure 2. $Wt1^{+/-}$ linked subfertility is associated with the abundance of a serine protease. (**A**) Average number of embryos and/or pups obtained from $Wt1^{+/+}$ and $Wt1^{+/-}$ mothers. 'n' within each bar represents the number of mice analyzed (mean ± s.e.m.) *$P < 0.05$, **$P < 0.01$, ***$P < 0.001$ as calculated by Student's *t*-test. (**B**) Percentage of the number of embryos retrieved at E3.5 from $Wt1^{+/+}$ ($n = 9$) and $Wt1^{+/-}$ ($n = 10$) mothers after wild type embryo transfer at E1.5. *$P < 0.05$ as calculated by Student's *t*-test. (**C**), Representative images of immuno-staining of the ampullary region of the oviduct from $Wt1^{+/+}$ females depicting Wt1 (red) and E-cadherin (green). Scale bars, 20 μm and 10 μm for the magnified image; DAPI, 4',6-diamidino-2-phenylindole. (**D**) Reduced Wt1 detected in the lower half of wild type mouse oviducts (n = 3 mice) when compared to the upper portions of mouse oviducts using a Wt1 antibody. Anti-Ldh: loading control. (**E**) Percentage of embryos during development cultured on wild type ($n = 75$ embryos) and *Wt1cKO* ($n = 95$ embryos) primary oviductal cells (pOCs) *ex vivo*. Two cells stage embryos were cultivated at day 0; day 1 represents percentage of embryos at 4-cell stage or higher, day 2 at morula and day 3 at blastocyst stage. Bars indicate mean ± s.e.m. *$P < 0.05$ as calculated by Student's *t*-test. (**F**) $Wt1^{+/+}$ (n = 2 mice; 23 embryos in total) and $Wt1^{+/-}$ (n = 4 mice; 21 embryos in total) E1.5 embryos were transferred to wild type pseudo-pregnant mice. Each bar denotes the percentage of embryos at each stage of development retrieved at E3.5 (mean ± s.e.m.). *$P < 0.05$ as calculated by Student's *t*-test. (**G**) Heat map of significantly altered extracellular proteins (Gene Ontology CC annotation based) when comparing oviductal fluid (OF) samples of $Wt1^{+/+}$ ($n = 3$) and $Wt1^{+/-}$ ($n = 3$) mice. Gene name, log2 fold change and p value from a two sided t-test are shown next to log2 LFQ (label-free quantification) intensities for the respective protein group. Clustering was done using Euclidean distance calculation in R. (**H**) Representative images of immuno-staining of the oviducts of $Wt1^{+/+}$ and $Wt1^{+/-}$ mice depicting Ovgp1 (red) and Prss29 (green). Scale bars, 20 μm; DAPI, 4',6-diamidino-2-phenylindole.

To assess the function of potential Wt1 binding elements within *Prss29*, we carried out reporter gene assays using two different fragments of *Prss29:* the 5' region (*pPrss29*) and an intronic region (*Prss29 I4*) (Fig. 3A), which were based on previous Wt1 ChIP-Seq analysis (4,19,20). To confirm the activity of Wt1 in regulating *Prss29*, we employed *Wt1cKO* pOCs that were co-transfected with Wt1 (*+Wt1*) or with an empty vector control (*-Wt1*). Here, we observed that transcriptional activity was

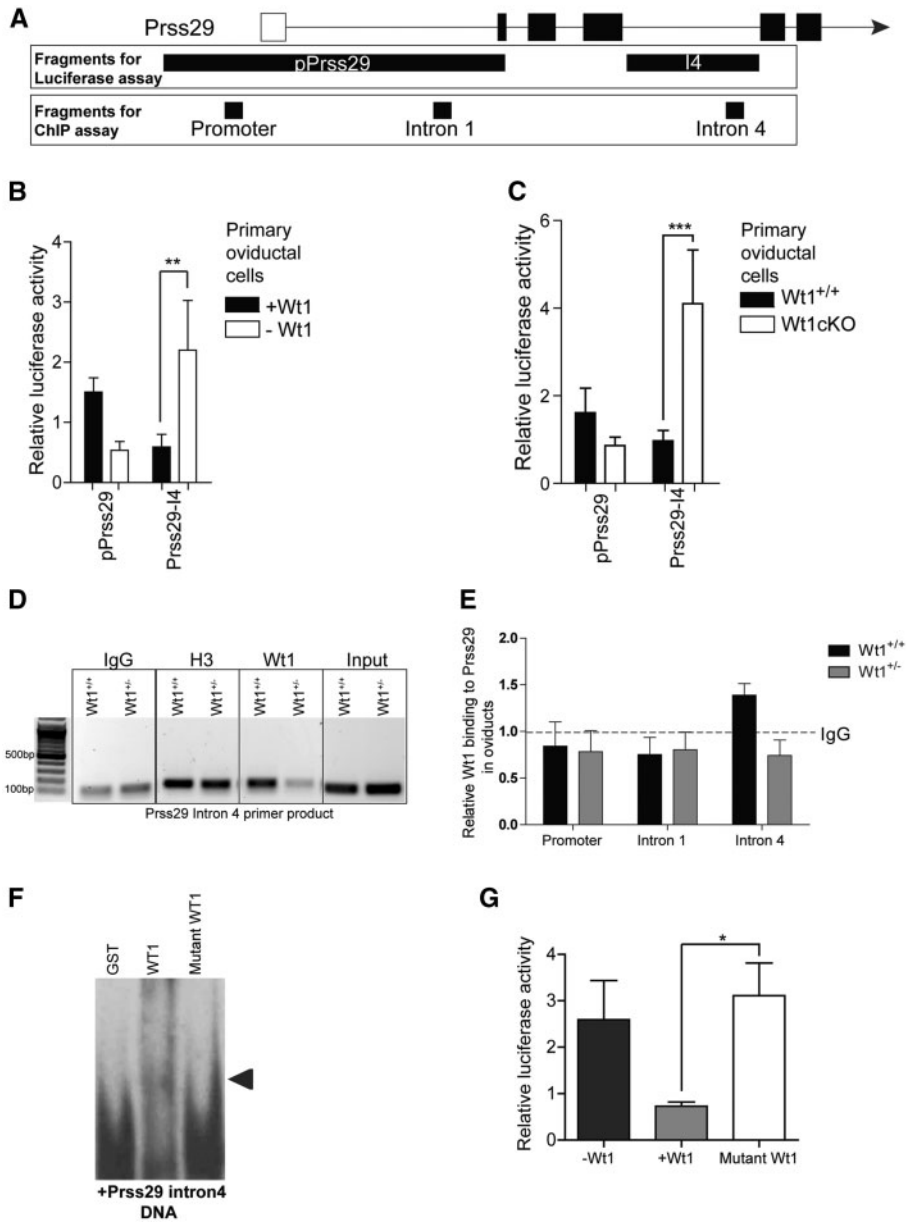

Figure 3. Wt1 binds to and represses *Prss29* expression. (**A**) Fragments of the *Prss29* genes used for luciferase assay (pPrss29 and I4) and ChIP-qPCR assay (promoter, intron 1 and intron 4). Filled boxes on the Prss29 gene encode coding exons, whereas exon 1 of *Prss29* (unfilled) is a non-coding exon. (**B**) Gene reporter assay in *Wt1cKO* pOCs co-transfected with either *Wt1* encoding or the blank *pRc/CMV* vector. PmaxGFP was used as a control for transfection efficiency. Cells were transfected with pGL3-pPrss29, pGL3-Prss29-I4 or pGL3 blank vectors. Luciferase activity of *Prss29* fragments were normalized to pGL3 blank vectors (mean ± s.e.m.). Data are representative of three independent experiments. $^{**}P < 0.01$ as calculated by two-way ANOVA and Bonferroni post-test. (**C**) Gene reporter assay in wild type and *Wt1cKO* pOCs transfected with pGL3-pPrss29, pGL3-Prss29-I4 or pGL3 blank vectors. PmaxGFP was used as a control for transfection efficiency. Luciferase activity of *Prss29* fragments were normalized to pGL3 blank vectors (mean ± s.e.m.). Data are representative of five independent experiments. $^{***}P < 0.001$ as calculated by two-way ANOVA and Bonferroni post-test. (**D**) Representative gel image of ChIP-DNA where bands represent amplicons of the *Prss29 intron* 4 region from $Wt1^{+/+}$ and $Wt1^{+/-}$ oviducts. DNA was isolated after ChIP with IgG, Histone H3 and Wt1 antibodies. Input control represents DNA that was not subjected to ChIP. Each band represents DNA isolated from 6 mice per genotype. (**E**) Relative Wt1 binding to regions of *Prss29* using $Wt1^{+/+}$ and $Wt1^{+/-}$ oviducts analysed by ChIP-qPCR assay. Binding assay using qPCR was normalized to IgG-antibody treated samples (set to 1; mean ± s.e.m.). Each bar represents fold enrichment from 2 independent experiments comprised of oviducts from 12 mice per genotype. The results were statistically not significant ($P > 0.05$) as calculated by Student's *t*-test. (**F**) Wt1 binding to the *Prss29* intron 4 region. Experiment as in 1C, but using the *Prss29* intron 4 region. (**G**), Gene reporter assay in *Wt1cKO* primary oviductal cells co-transfected with either *Wt1*, mutant *Wt1* (R413M) or the blank *pRc/CMV* vector. PmaxGFP was used as a control for transfection efficiency. Cells were transfected with pGL3-Prss29-I4 or pGL3 Promoter as reporter vectors. Luciferase activity of *Prss29* intron 4 fragment was normalized to pGL3 Promoter vector (mean ± s.e.m.). Data are representative of four independent experiments. $^{*}P < 0.05$ as calculated by one-way ANOVA and Dunnett's multiple comparison post-test.

increased in cells lacking Wt1, mediated by the *Prss29 I4* fragment (Fig. 3B), while *pPrss29* did not significantly change transcriptional activity. This effect could also be recapitulated when using pOCs from wild type and *Wt1cKO* mice without Wt1 co-transfection (Fig. 3C). To confirm Wt1 binding to *Prss29 in vivo*, we performed ChIP on oviducts from adult $Wt1^{+/+}$ and $Wt1^{+/-}$mice. ChIP-PCR revealed that DNA precipitated by anti-Wt1 antibody showed increased binding to the *Prss29 I4*

fragment in wild type mice, when compared to $Wt1^{+/-}$oviducts (Fig. 3D). ChIP-qPCR also showed increased binding of Wt1 to the *Prss29 I4* fragment in wild type mice, when compared to the promoter and intron 1 regions of *Prss29* (Fig. 3E). In order to see whether the strain specific subfertility could be attributed to differences in the Wt1 binding region within *Prss29*, we sequenced the *Prss29 intron* 4 fragments from the different strains. Indeed, the B6 sequence deviated from the MF1 and 129Sv sequence in that it was longer and had more repeat sequences (Supplementary Material, Fig. S6F).

When using the *Prss29* intron 4 sequence from the MF1 strain as a target for WT1 binding in EMSA studies, we observed reduced DNA binding of the Wt1-R413M protein (Fig. 3F). Similarly, the transcriptional repression mediated by the *Prss29* intron 4 fragment was found to be lost when co-transfecting *Wt1cKO* pOCs with the Wt1-R413M encoding plasmid (Fig. 3G). This reiterates our finding that WT1-R413M is a loss-of-function variant.

Prss29 activity affects integrity of early embryos

Since our data showed that Prss29 was upregulated in $Wt1^{+/-}$ oviducts, we aimed to understand the consequence of precocious Prss29 activity for embryo development, both *in vivo* and *in vitro*. We cultured two-cell stage wild type embryos with increasing amounts of recombinant Prss29 protein (3–300ng/ml) or a catalytically inactive form of rPrss29. Notably, increasing concentrations of rPrss29 negatively affected the percentage of blastocysts, a phenomenon that was significantly different to that of the catalytically dead Prss29 (Fig. 4A). When we increased the concentration of rPrss29 even further (1 μg/ml), we observed preimplantation embryos lacking their zona pellucida, a protective glycoprotein matrix that surrounds the embryo until implantation (21) (Fig. 4B). This effect was not seen when embryos were cultured in the presence of mutant rPrss29. Since the ZP is sensitive to protease-mediated cleavage, we analysed the integrity of the ZP of embryos from $Wt1^{+/-}$ oviducts (22). Consistent with increased ZP digestion in high concentrations of rPrss29, E0.5 embryos from $Wt1^{+/-}$ oviducts dissolved quicker than embryos from wild type oviducts when subjected to *in vitro* protease digestion (Fig. 4C). Shorter digestion time was accompanied by swelling and lysis of embryos from $Wt1^{+/-}$ oviducts (Supplementary Material, Fig. S7A). These findings suggest that the $Wt1^{+/-}$ oviductal microenvironment affected ZP structure and integrity due to premature Prss29 activity.

Based on our observations that exposure of embryos to Prss29 interferes with embryo development, we asked whether

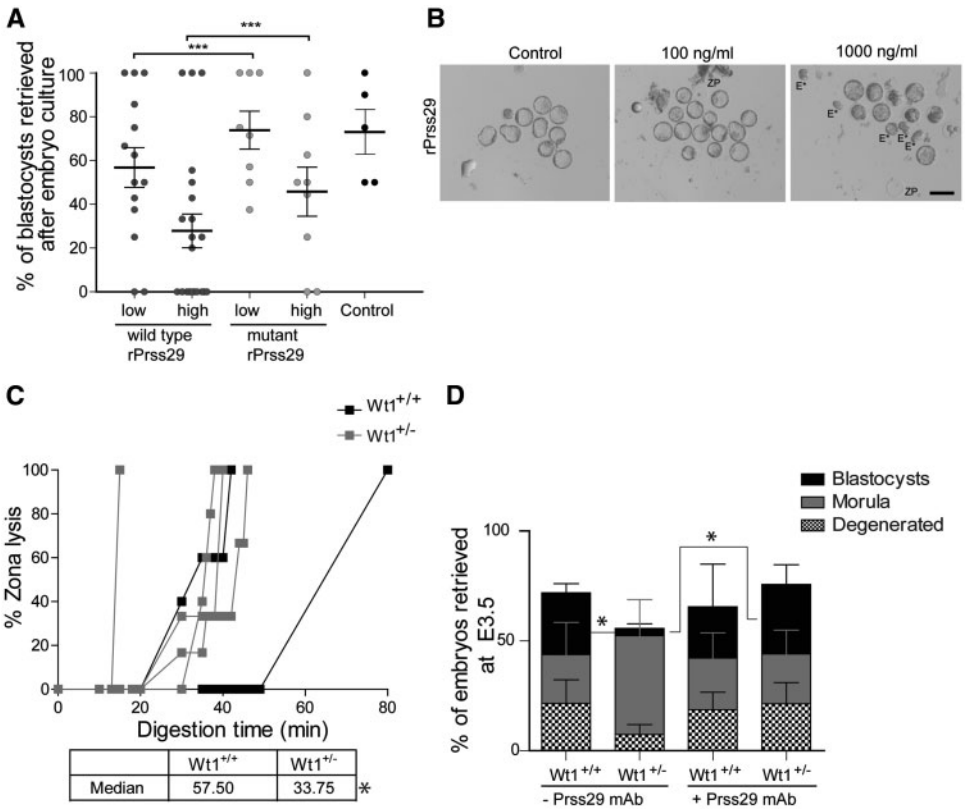

Figure 4. Prss29 is a causative factor of *Wt1* heterozygosity-mediated subfertility. (**A**) Wild type E1.5 embryos incubated in increasing concentrations of rPrss29, mutant rPrss29 or control media only. Each dot represents a single experiment showing the percentage of blastocysts observed at E3.5, when cultured in low (3 ng/ml, 10 ng/ml and 30 ng/ml; rPrss29 $n = 70$ embryos; mutant rPrss29 $n = 46$ embryos) or high (100 ng/ml and 300 ng/ml; rPrss29 $n = 59$ embryos; mutant rPrss29 $n = 39$ embryos) recombinant protease. Error bars indicate s.e.m. *** $P < 0.001$ as calculated by one-way ANOVA and Tukey's multiple comparison post-test. (**B**) Representative images of embryos cultured in control media, 100 ng/ml or 1 μg/ml of rPrss29. ZP, remnant zona pellucida; E*, lysed embryos with dis-integrated blastomeres lacking zona pellucida; Scale bar, 1000 μm. (**C**) Percentage of zona pellucida lysis over time in E0.5 embryos obtained from $Wt1^{+/+}$ and $Wt1^{+/-}$ oviducts when incubated in 1% α-chymotrypsin. Each line represents data from one mouse ($Wt1^{+/+}$ $n = 2$ mice; $Wt1^{+/-}$ $n = 4$ mice). *$P < 0.05$ for medians between each group calculated by Student's *t*-test. (**D**) Wild type E1.5 embryos were transferred to $Wt1^{+/+}$ and $Wt1^{+/-}$ pseudo-pregnant mice, with or without a monoclonal Prss29 antibody (Prss29mAb). Each bar denotes the percentage of embryos at each stage of development retrieved at E3.5 (mean ± s.e.m.). Each embryo stage was compared with each other (i.e, blastocyst from column 1 is significantly different to column 2; blastocysts from column 2 are significantly different to column 4). Number of total embryos per column is as follows: Column 1 = 32; Column 2 = 49; Column 3 = 47; Column 4 = 55. *$P<0.05$ as calculated by Student's *t*-test.

using an antagonistic antibody against Prss29 would be sufficient to rescue the Wt1-mediated subfertility *in vivo*. We injected the anti-Prss29 antibody (17) (Prss29 *mAb*) together with E1.5 wild type embryos into the oviductal lumen of $Wt1^{+/+}$ and $Wt1^{+/-}$ females and retrieved them two days later. In the absence of Prss29 *mAb*, fewer blastocysts could be retrieved from $Wt1^{+/-}$, recapitulating our previous observations (Fig. 4D). This effect could be corrected by neutralizing Prss29 on two levels, improved cleavage rate (Supplementary Material, Fig. S7B) as well as the increase in the total number of embryos retrieved (Fig. 4D). Therefore, blocking Prss29 activity in the oviduct was sufficient to rescue the subfertility in $Wt1^{+/-}$mice.

Discussion

Mutations in *WT1* leading to Wilms tumour may either be somatic (∼97%) or germline (∼3%) (23,24). WAGR syndrome (deletion of PAX6 and WT1 genes among others), Denys–Drash syndrome (missense mutation in exons 8 and 9 of WT1) and Frasier syndrome (mutations in exons 8, 9 and intron 9 of WT1) are all results of germline mutations. In our study, one patient was identified with the missense mutation, R413M, resulting in a WT1 protein with reduced DNA binding. Although this heterozygous missense variation has not yet been characterized, it is possible that this mutation can affect WT1's function as a transcription factor. It has been shown that for transcription factor Sp1, mutation of a single amino acid Alanine on the DNA-recognition helix, affects the binding mode of all three zinc fingers (25). The impact of the R413M mutation was predicted as 'non-neutral' by SNAP (26), indicating that the resulting point mutation functionally affects the protein. The manifestation of infertility in the R413M patient can be possibly due to a dominant negative function of WT1 similar to Denys-Drash syndrome, where the mutant WT1 renders the wild-type protein inactive, resulting in a protein defective in DNA binding (27,28). This point is further supported by our gene reporter assays where the R413M mutation within Wt1 affects the repression of *Prss29*.

By using $Wt1^{+/-}$ mice as a model to study Wt1's role in maintaining female fertility, we confirmed that the subfertility was due to an oviductal defect and not due to underlying ovarian effects. Our experiments show that primary oviductal cells lacking *Wt1* were inferior to wild type cells in their ability to support preimplantation embryo development *ex vivo*. This supports our findings that the oviductal environment is altered upon loss of Wt1, prompting us to look deeper into the components of the oviductal fluid. By performing a proteomic approach to compare oviductal fluids from wild type and $Wt1^{+/-}$ mice, we found a serine protease, Prss29, which was restricted to $Wt1^{+/-}$ oviductal fluid, and three down-regulated serine protease inhibitors, Itih1, Itih2 and Serping1. When comparing this data to our microarray data from whole oviductal tissue, we find that *Prss29* was also upregulated in $Wt1^{+/-}$ mice. *Prss29* is an implantation serine protease known to degrade the ECM during uterine implantation (16). *Itih1* and *Itih2* belong to the inter-α-inhibitor family and are involved in ECM stabilization by directly binding to hyaluronic acid (29). MMP2, a matrix metalloproteinase, is required for the breakdown of the zona pellucida ECM (30), while also being required for human embryo implantation, by participating in the embryonic trophoblast invasion (31). These functions provide a strong hint toward the inhibitors working together with Prss29 during early pregnancy.

Treating pre-implantation embryos with increasing concentrations of recombinant Prss29 was deteriorative for preimplantation embryo development as observed by fewer blastocysts and some embryos even lacking their zona pellucida. Therefore, it is highly likely that Prss29 causes pre-mature digestion of the zona pellucida of preimplantation embryos, while still in the oviduct. We tested this by incubating E0.5 embryos from $Wt1^{+/+}$ and $Wt1^{+/-}$ mice in 1% α-chymotrypsin, where embryos from the $Wt1^{+/-}$ mice dissolved quicker than embryos from wild type females. The data propose that early embryos without their zona pellucida, whilst in the $Wt1^{+/-}$ oviducts, might be disintegrated or be attacked by the maternal immunological system or even attempt to implant in the oviduct (known as tubal pregnancy). Even though tubal pregnancies in mice are extremely rare (32), tubal pregnancies are observed in 1–2% of all human pregnancies (33). The subfertility phenotype in $Wt1^{+/-}$ mice could be reversed by blocking Prss29 activity in the oviducts with the help of an antagonistic antibody. The blocking antibody was beneficial in increasing blastocyst numbers, ascertaining a direct link between Prss29 and deteriorative pre-implantation embryo development.

Wt1 dichotomously regulates transcription resulting in either activation or repression of its target genes (34). For example, *Pax2* (paired box 2) is repressed by Wt1 during kidney development (35), whereas *Amhr2* (Anti müllerian hormone receptor 2) is activated by Wt1 (36). Our data suggest that *Prss29* is repressed by Wt1 in wild type oviducts, by binding to an intronic region. Control of gene expression by binding to intronic sequences has been shown where the transcription of two promoter regions (*Angiogenin* and *Ribonuclease 4*) is influenced by the formation of a CTCF-dependent chromatin loop in an intronic region containing insulators (37). Additionally, ChIP-seq analysis on podocytes revealed that Wt1 binds to intron 3 of the Bmp inhibitor encoding gene, *Bmper*, resulting in its transcriptional activation (19).

Our data also show that $Wt1^{+/-}$ females on the 129/Sv (MF1) background are infertile, while they are subfertile on the MF1 background. However, mice on the B6 background were fertile. When counting oocyte numbers, we observe a similar reduction in $Wt1^{+/-}$ mice between all three mouse strains, although fertility in $Wt1^{+/-}$ (B6) mice was not compromised. Similarly, Prss29 was localized only to $Wt1^{+/-}$mice of 129/Sv (MF1) and MF1 backgrounds, where fertility was compromised. Strain specific derepression of *Prss29* by Wt1 can be attributed to altered binding affinity in different mouse strains due to changes in enhancer regions, altered expression of down-stream genes, or disruption of topologically associated domains (38), all affecting transcription by Wt1. In fact, by sequencing the *Prss29* intron 4 region of three different mouse strains, we observed variations in the region harboring the potential Wt1 binding motifs, specifically varying numbers of repeat sequences.

Here, we report a novel role for the Wilms tumor protein Wt1 in fertility. Reduction of Wt1 activity leads to enhanced protease and decreased protease inhibitor levels in the oviduct. Molecularly, Wt1 prevents oviductal expression of *Prss29* encoding a protease with a role in implantation. This highlights the importance of maintaining proteostasis for preimplantation development and suggests a role for Wt1 as a 'proteostat'. Of note, also the estrogen receptor has been identified as a regulator of oviductal proteostasis (39). These recent data as well as our data suggest that anti-protease antibody or protease inhibitor administration might provide an active contribution towards treatment of female patients suffering from infertility.

Materials and Methods

DNA isolation and *WT1* sequencing

Whole blood was drawn from infertile patients at the Department of Gynecological Endocrinology and Fertility

Disorders, University Hospital Heidelberg, where Institutional Review Board approval was obtained from all recruitment, laboratory, and data management sites. Written informed consent was obtained from study subjects. Known risk factors for female and male fertility were excluded. DNA from whole blood was isolated using buffy coat extraction by adding an equal volume of sterile PBS and centrifuging at 2000 rcf for 20 min followed by plasma removal. DNA was isolated from the interphase using the QIAamp DNA Mini Kit (Qiagen), and the DNA concentration was adjusted to 50 ng/µl.

PCR was performed using a total of 11 primer pairs were used to amplify all ten exons of *WT1*. In order to distinguish between the sequences of patients, each primer-patient combination had specific indices added to both primers. The PCR product pools were cleaned up using the Gel and PCR Clean-up kit (Macherey-Nagel). The cleaned products were sequenced at the Sequencing facility in FLI, Jena using the MiSeq, alignment using the GRCh38/hg38 genome and variant analysis using the CLC workbench.

Gel shift assay

Using the site-directed mutagenesis kit (Stratagene), the R413M mutation was introduced in the pGEX1 vector harboring the four zinc fingers of Wt1 (-KTS). The mutagenesis was confirmed by sequencing. Recombinant, bacteria expressed glutathione S-transferase (GST) fusion proteins of Wt1 (-KTS) and mutant R413M Wt1 (-KTS) were purified as previously described (40). *Egr1* DNA (30 bp) and *Prss29 intron4* DNA (133 bp) fragments were ordered as a single oligonucleotide and annealed together. Gel shift assays were carried out using the DIG Gel shift kit, 2nd generation (Roche).

Mice

Wt1 heterozygous ($Wt1^{+/-}$) mice were maintained on the *MF1*, *B6* or *129Sv* strains by crossing $Wt1^{+/-}$ males with wild type females. For plug mating analysis, females of specific genotypes were housed with wild type males and were checked every morning for the presence of a plug. For embryo analysis, female mice were harvested at specific time points during preimplantation embryo development and their oviducts were flushed from the infundibulum in order to collect developing embryos. Typically, female mice between 2 and 6 months were used.

Conditional Wt1 knockout mice were generated by breeding $Wt1^{fl_{ox}/fl_{ox}}$ females (41) to Rosa26CreER^{T2} males (42). All mice were bred and maintained in the Animal Facility of the Leibniz Institute on Aging – Fritz Lipmann Institute (FLI), Jena, Germany, according to the rules of the German Animal Welfare Law. Gender- and age-matched mice were used whenever possible. Animals were housed under specific pathogen-free conditions (SPF1) and maintained on a 12-h light/dark cycle and were fed with mouse chow and tap water *ad libitum*.

Primary oviduct cell culture

Oviducts were dissected, washed in PBS and minced in a solution containing Collagenase A (10 ng/µl) and DNase I (10 ng/µl) in 500 µl sterile PBS for 1 h at 37 °C at 800 rpm. The digested tissue was passed through a 70 µm cell strainer (BD Biosciences), flow through centrifuged and the cell pellet washed twice. Up to $3*10^5$ cells could be obtained from two oviducts. After washing, the cell pellet was suspended in pre-warmed cell culture media (DMEM F12 (Gibco) + 2% FCS, ZellShield (Minerva Biolabs) and Reno supplement (Promocell)) and transferred onto gelatin-coated 12-well plates. The cells were left undisturbed for three days to allow cell attachment at 37 °C, 5% CO_2 and 95% humidity, followed by media change.

In case of cells isolated from conditional knockout mice, the cells were treated after 3 days in culture with 2 µM 4'-OH tamoxifen for 3 days at 37 °C, 5% CO_2 and 95% humidity, to allow *Cre*-mediated recombination. Cells were further propagated and maintained until 7 divisions *in vitro*.

Embryo co-culture

For embryo culture on primary oviductal cells, the cells were split two days prior to culture into a 24-well plate. Five hours prior to culturing embryos, the media of wells containing the cell monolayers were replaced with KSOM (MR-121-D; Millipore) and maintained at 37 °C, 5% CO_2 and 95% humidity. Two-cell staged embryos (E1.5) in groups of 4–8 embryos were cultured in each well. The numbers of degenerated embryos, morulae and blastocysts were recorded for three consecutive days.

Embryo transfer

Wild type (NMRI) E1.5 embryos were transferred to oviducts of pseudo pregnant (females mated with vasectomized males) wild type and $Wt1^{+/-}$ (MF1) mice at E1.5. Embryos were analyzed for their development at E3.5 or for the number of pups at P0.

In case of heterozygous embryo transfer experiments, E1.5 embryos from wild type and $Wt1^{+/-}$ (MF1) females were transferred to wild type (NMRI) pseudo pregnant females, and analyzed for their development at E3.5.

For embryo transfer along with Prss29 monoclonal antibody, E1.5 wild type (NMRI) embryos were transferred into pseudo pregnant wild type and $Wt1^{+/-}$ (MF1) mice along a solution of 2–5 µl of Prss29 monoclonal antibody supernatant (stock concentration: 5 µg/ml). The control group, without Prss29 mAb, was injected with wild type embryos alone. Embryos were analyzed for their development at E3.5.

Zona pellucida digestion assay

Zona pellucida lysis *in vitro* was compared between E0.5 embryos obtained from natural mating of $Wt1^{+/+}$ and $Wt1^{+/-}$ females with wild type males. Embryos were cultured in 1% α-chymotrypsin in PBS under mineral oil and the embryos were observed under a light microscope at 5–10 min intervals until all zones were completely lysed.

Immunohistochemistry

Oviducts from mouse and human were isolated, washed with 1x PBS, fixed in 4% PFA overnight at 4°C, embedded in paraffin and stained as previously mentioned using mouse anti-Wt1 (6F-H2; Dako), rabbit anti-Ovgp1 (M90; sc-48754; Santa Cruz), rabbit anti-E-cadherin (24E10; #3195; Cell Signaling) or mouse anti-Prss29 (17). After overnight incubation at 4 °C and washing with 1x PBS, the slides were incubated with Alexa Fluor® secondary antibodies (488/546/594; Invitrogen) for 1 h at room temperature in the dark. After further washes, the slides were treated with Hoechst 33342 (1:100) in 1x PBS for 10 min for DNA visualization, and mounted in Prolong® Gold AntiFade reagent (Life Technology) sealed with coverslips. Sections were analyzed and

imaged with a Zeiss Axio Apotome 2 microscope and the corresponding AxioVison software.

Immunoblotting

Oviductal tissue from mouse and human were minced and lysed in RIPA buffer (50 mM Tris pH 7.5; 150 mM NaCl; 0,1% SDS) containing protease Inhibitors at 4 °C (Roche), followed by centrifugation for 1 min at full speed. The flow through was collected and protein concentration measured by Bradford assay. 30 μg of total protein was used for Western blotting as described previously (36) using rabbit anti-Wt1 (C19; Santa Cruz), mouse anti-Prss29 (17) or goat anti-Ldh (ab2101; Abcam). After washes in 1x-TBS-Tween20, the membrane was incubated in anti-mouse/rabbit/goat-HRP coupled secondary antibodies (Dako) for 1 h at room temperature. The membrane was washed thrice in 1x-TBS-Tween20, followed by detection using Pierce ECL Western Blotting Substrate (Thermo Scientific). The signals were developed on X-ray films and recorded with the Epson Perfection 4870 scanner.

Mass spectrometry

The oviducts from three mice per genotype (wild type and $Wt1^{+/-}$ (MF1)) were obtained at E2.5 by mating with vasectomized males. Oviducts were flushed, the flushing was spun down and the supernatant was considered as oviductal fluid, thereby removing epithelial cell contamination. Samples were concentrated and desalted using a Centricon centrifugal filter with a 3 kDa cutoff (Merck Millipore). The eluate was resolved by SDS-PAGE and stained with Simply Blue Safe Stain (Invitrogen). In-Gel digestion was performed accordingly to the previously published protocol (43). In brief, excised gel bands were washed several times with Ammonium bicarbonate buffer; proteins were reduced by DTT and alkylated by IAA. A 12 ng/μl Trypsin solution was used to perform in-gel digestion overnight. Generated peptides were extracted by an increasing content of Acetonitrile. Prior to LC-MS/MS analysis, peptides were desalted by the Stop-and-Go technique (44).

Liquid Chromatography and mass spectrometer instrumentation consisted of a nanoLC (Thermo Scientific) coupled via a nano-electrospray ionization source to an ion-trap based LTQ Velos XL instrument (Thermo Scientific). Peptide separation was carried out according to their hydrophobicity on an in-house packed 20 cm column with 3.0 μm C18 beads (Dr Maisch GmbH) using a binary buffer system consisting of solution A: 0.5% acetic acid and B: 80% acetonitrile, 0.5% acetic acid. Linear gradients from 7–38% B in 130 min were applied with a following increase to 80% B within 5 min and a re-equilibration to 5% B. MS spectra were acquired at a resolution of 30,000 at 400 m/z after accumulation of 1E6 ions (AGC target) within a maximal injection time of 60 ms. Top 15 method was applied for MS/MS spectra at a resolution of 7,500 at 400 m/z. AGC target and maximal injection time were set to 1E4 and 30 ms, respectively. The isolation window was 2 m/z and activation time was set to 10 ms. A normalized collision energy of 35 was used for CID fragmentation.

The raw data were processed with MaxQuant (1.3.3.4) and the implemented Andromeda Search engine. MS/MS spectra were correlated to the reference mouse database. Mass tolerance settings were set as by default, the minimal peptide length was 7 amino acids and the FDR was controlled by the decoy database approach at the peptide-spectrum-match and protein level to 1%. In total, a maximum of two miss cleavages were allowed under tryptic conditions. Match between runs, label free quantification and re-quantification algorithms were enabled.

LFQ intensities were $\log_2$ transformed and the ratio of $Wt1^{+/+}$/$Wt1^{+/-}$ was calculated as the difference of $\log_2$ LFQ intensities means for each replicate. A two-tailed t-test was applied to identify significant regulated proteins. Proteins showing a greater absolute fold-change of 2 and a p-value < 0.05 were considered as biological significant candidates. To include proteins that are exclusively for one of the genotypes, missing data were replaced by random data from a down-shifted Gaussian distribution (width = 0.5, downshift: 1.8) mimicking the detection limit of the mass spectrometer. Note that only proteins that were quantified at least 2 times in one the genotypes were included and Gaussian distribution was verified by histogram analysis of $\log_2$ LFQ intensities. Among the significant proteins, a further selection for secreted proteins was performed according to annotation based gene ontology (cellular component), to rule out contamination of the mucosal epithelium.

mRNA isolation, cDNA synthesis and qPCR analysis

Total RNA was isolated from the oviducts using the phenol-chloroform method (45). cDNA was synthesized using 500 ng RNA with the iScript™ cDNA synthesis kit (BioRad). Quantitative real time PCR was measured in triplicates using 12 ng cDNA on the CFX384 Touch real-time PCR detection system (BioRad). The data were analyzed by the delta delta Ct method (46).

Microarray

The microarray analysis was performed using a Mouse Genome 430 2.0 Array from Affymetrix. Entire oviductal tissue at E2.5 from three pseudo-pregnant mice each from $Wt1^{+/+}$and $Wt1^{+/-}$ genotypes were used for RNA isolation. The integrity of each RNA sample was checked with a RNA 6000 Nano chip (Agilent) and 1 μg total RNA per sample was used. The RNA samples were subjected to reverse transcription, second strand synthesis, phenol-chloroform extraction, ammonium acetate precipitation, *in vitro* transcription, cRNA synthesis with biotinylation, cRNA purification, cRNA fragmentation, hybridization, staining of the hybridized cRNA and scanning of the chip. Probe set IDs from Affymetrix were retrieved, averages calculated from all three samples per genotype, fold change ($Wt1^{+/-}$/$Wt1^{+/+}$), and a two-tailed t-test was calculated. Genes that showed a high variance in their signal between samples and genes that were expressed at low levels (signal strength < 30) were eliminated. Differentially expressed genes were generated using an FDR < 0.05, and unannotated genes were omitted.

Chromatin immunoprecipitation

Oviducts were isolated from adult $Wt1^{+/+}$ and $Wt1^{+/-}$mice, washed and minced in a solution containing Collagenase A (10 ng/μl) for 1 h at 37 °C at 500 rpm. The tissue was passed through a 70μm cell strainer (BD Biosciences), flow through centrifuged and the cell pellet was washed. Protein-DNA complexes were fixed in 1% formaldehyde for 8 min at room temperature, quenched using 125 mM glycine, resuspended in chromatin immunoprecipitation (ChIP) buffer (50 mM Tris HCl pH 7.5, 150 mM NaCl, 5mM EDTA, 0.1% SDS, 1.0% TritonX100) containing protease inhibitors (Roche), and sonicated for 30 cycles

(15 seconds on/off). The chromatin was immuno-precipitated using rabbit anti-Wt1 (C19; Santa Cruz), rabbit anti-IgG (I5006; Sigma) and rabbit anti-Histone H3 (ab1791; Abcam) antibodies as previously described (4). The antibody-protein-DNA complexes were eluted, reverse cross-linked, protein digested and DNA was isolated using the Phenol-Chloroform method (45). DNA was amplified either by qPCR (ChIP-qPCR) or conventional PCR (ChIP-PCR) for regions of *Prss29* (promoter: 130 bp, intron 1: 171 bp and intron 4: 133 bp). The qPCR program was run using the CFX384 Touch real-time PCR detection system (Bio-Rad). The data were analyzed by the delta delta Ct method (46).

Luciferase reporter assay

PCR amplification of the *Prss29* fragments was performed with the KOD polymerase kit (Novagen). The fragments were ligated into the *pGL3* (Basic/Promoter) vectors (Promega). Inserts were confirmed by sequencing. Positive clones were propagated and stored at a concentration of 1 μg/μl. Primary oviductal cells were transfected using Amaxa™ Basic Nucleofector™ Kit for Primary Mammalian Epithelial Cells (Lonza). Briefly, the cell suspension in transfection reagent along with 1 μg of pGL3-*Prss29* (pPrss29: 2402 bp and I4: 857 bp) reporter constructs, 1 μg of mouse Wt1 (-KTS) expression plasmid and 50 ng of pGL4.74 were co-transfected in Amaxa cuvettes using the 'U017' program. After transfection, the cell mixture was transferred to a 24-well plate, grown for 48 h after which the Firefly/Renilla ratio was measured using the Dual-Luciferase Assay kit (Promega) on a Mithras LB940 plate reader (Berthold). Values were normalized to either empty pGL3 reporter plasmids (for Prss29 constructs) or RcCMV expression plasmid (for Wt1 expression).

For the Wt1-R413M experiments, the R413M mutation (CGG > ATG) was introduced into murine Wt1 using the site-directed mutagenesis kit (Stratagene) and the Wt1(-KTS) encoding vector. Successful mutagenesis was confirmed by sequencing.

Sequencing of *Prss29* Intron 4 from different mouse strains

Genomic DNA from oviducts from wild type *MF1*, *B6* or *129Sv* strains were isolated using QIAamp DNA Mini kit. PCR amplification of the *Prss29 I4* fragments was performed with the KOD polymerase kit (Novagen). The fragments were ligated into the *TOPO* vector (Invitrogen) and the inserts were confirmed by sequencing.

rPrss29 embryo culture

Working concentration (1 μg/ml) of rPrss29 (CSB-MP859566MO; Cusabio) and rPrss29 S228A were prepared from the original stock (0.1 mg/ml) by dissolving in KSOM media. Droplets of varying concentrations (3, 10, 30, 100, 300 and 1000 ng/ml) in 40 μl were placed on a dish covered with mineral oil (embryo culture tested; Sigma). KSOM medium was used as the diluent. Embryos cultured only in KSOM were used as control. Groups of two-cell staged embryos were cultured in droplets (not exceeding 8 embryos per droplet). The embryos were cultured at 37 °C, 5% CO_2 and 95% humidity for two more days and the numbers of degenerated embryos, morulae and blastocysts were recorded.

Primers

The primers used in this study can be found in Supplementary Material, Table S3.

Statistics

Group sizes were determined based on preliminary experiments. No statistical method was used to predetermine the sample size. No animals were excluded from the analysis. Mice were assigned at random to groups and animal experiments were not blinded. Statistical significance was determined using two-tailed unpaired Student's *t*-test, under the untested assumption of normality. There was an estimate of variation between groups, and the variance was similar. Data were analyzed using GraphPad prism version 5.0. All data are presented as mean ± s.e.m. and evaluated for statistical significance ($P < 0.05$).

Supplementary Material

Supplementary Material is available at *HMG* online.

Acknowledgements

We thank Udo Markert for discussions throughout the project and contact to the Clinics; Manfred Gessler for providing primer sequences for *WT1* exon sequencing and critical reading of the manuscript; Markus Hildner and Christine Ströhl for assistance with the microarray experiments; Derrick Rancourt for providing Prss29 antibody; the FLI Animal facility staff, in particular Dominique Galendo, Frank Kaufmann and Jenny Buchelt; Lihua Dong for discussion and review of the manuscript; Tom Bates for review of the manuscript; Eric Donahue for help with statistical analysis; Nina Kreuzenbeck for strain specific sequencing analysis and Gabriele Günther for technical assistance. The authors would like to thank the Exome Aggregation Consortium and the groups that provided exome variant data for comparison.

Author Information

The microarray data discussed in this publication have been deposited in NCBI's Gene Expression Omnibus (47) and are accessible through GEO Series accession number GSE75924 (http://www.ncbi.nlm.nih.gov/geo/query/acc.cgi?acc=GSE75924). The mass spectrometry proteomics data have been deposited to the ProteomeXchange Consortium (48) via the PRIDE partner repository with the dataset identifier PXD003283.

Conflict of Interest statement. None declared.

Funding

This work was funded by the Leibniz Association and a grant from the Else Kröner-Fresenius-Stiftung to C.E. Funding to pay the Open Access publication charges for this article was provided by the Leibniz Association.

References

1. Forti, G. and Krausz, C. (1998) Clinical review 100: Evaluation and treatment of the infertile couple. *J. Clin. Endocrinol. Metabol.*, **83**, 4177–4188.

2. Rackley, R.R., Flenniken, A.M., Kuriyan, N.P., Kessler, P.M., Stoler, M.H. and Williams, B.R. (1993) Expression of the Wilms' tumor suppressor gene WT1 during mouse embryogenesis. *Cell Growth Differ.*, **4**, 1023–1031.
3. Chau, Y.Y., Brownstein, D., Mjoseng, H., Lee, W.C., Buza-Vidas, N., Nerlov, C., Jacobsen, S.E., Perry, P., Berry, R., Thornburn, A., *et al.* (2011) Acute multiple organ failure in adult mice deleted for the developmental regulator Wt1. *PLoS Genet.*, **7**, e1002404.
4. Dong, L., Pietsch, S., Tan, Z., Perner, B., Sierig, R., Kruspe, D., Groth, M., Witzgall, R., Grone, H.J., Platzer, M., *et al.* (2015) Integration of cistromic and transcriptomic analyses identifies Nphs2, Mafb, and Magi2 as Wilms' Tumor 1 target genes in podocyte differentiation and maintenance. *J. Am. Soc. Nephrol.*, **26**, 2118–2128.
5. Kreidberg, J.A., Sariola, H., Loring, J.M., Maeda, M., Pelletier, J., Housman, D. and Jaenisch, R. (1993) WT-1 is required for early kidney development. *Cell*, **74**, 679–691.
6. Kreidberg, J.A., Natoli, T.A., McGinnis, L., Donovan, M., Biggers, J.D. and Amstutz, A. (1999) Coordinate action of Wt1 and a modifier gene supports embryonic survival in the oviduct. *Mol. Reprod. Dev.*, **52**, 366–375.
7. Stewart, C.A. and Behringer, R.R. (2012) Mouse oviduct development. *Results Probl. Cell Differ.*, **55**, 247–262.
8. Aviles, M., Gutierrez-Adan, A. and Coy, P. (2010) Oviductal secretions: will they be key factors for the future ARTs?. *Mol. Hum. Reprod.*, **16**, 896–906.
9. Leese, H.J., Hugentobler, S.A., Gray, S.M., Morris, D.G., Sturmey, R.G., Whitear, S.L. and Sreenan, J.M. (2008) Female reproductive tract fluids: composition, mechanism of formation and potential role in the developmental origins of health and disease. *Reprod. Ferti. Dev.*, **20**, 1–8.
10. Wang, H., Li, G., Zhang, J., Gao, F., Li, W., Qin, Y. and Chen, Z.J. (2015) Novel WT1 missense mutations in Han Chinese women with premature ovarian failure. *Sci. Rep.*, **5**, 13983.
11. Gao, F., Zhang, J., Wang, X., Yang, J., Chen, D., Huff, V. and Liu, Y.X. (2014) Wt1 functions in ovarian follicle development by regulating granulosa cell differentiation. *Hum. Mol. Genet.*, **23**, 333–341.
12. Rauscher, F.J., 3rd, Morris, J.F., Tournay, O.E., Cook, D.M. and Curran, T. (1990) Binding of the Wilms' tumor locus zinc finger protein to the EGR-1 consensus sequence. *Science*, **250**, 1259–1262.
13. Pelletier, J., Schalling, M., Buckler, A.J., Rogers, A., Haber, D.A. and Housman, D. (1991) Expression of the Wilms' tumor gene WT1 in the murine urogenital system. *Genes Dev.*, **5**, 1345–1356.
14. Oon, V.J. and Johnson, M.R. (2000) The regulation of the human corpus luteum steroidogenesis: a hypothesis?. *Hum. Reprod. Update*, **6**, 519–529.
15. Buhi, W.C., Alvarez, I.M. and Kouba, A.J. (2000) Secreted proteins of the oviduct. *Cells, Tissues, Organs*, **166**, 165–179.
16. O'Sullivan, C.M., Liu, S.Y., Rancourt, S.L. and Rancourt, D.E. (2001) Regulation of the strypsin-related proteinase ISP2 by progesterone in endometrial gland epithelium during implantation in mice. *Reproduction*, **122**, 235–244.
17. Sharma, N., Liu, S., Tang, L., Irwin, J., Meng, G. and Rancourt, D.E. (2006) Implantation Serine Proteinases heterodimerize and are critical in hatching and implantation. *BMC Dev.Biol.*, **6**, 61.
18. Huang, Z.P., Yu, H., Yang, Z.M., Shen, W.X., Wang, J. and Shen, Q.X. (2004) Uterine expression of implantation serine proteinase 2 during the implantation period and in vivo inhibitory effect of its antibody on embryo implantation in mice. *Reprod. Fertil. Dev.*, **16**, 379–384.
19. Motamedi, F.J., Badro, D.A., Clarkson, M., Lecca, M.R., Bradford, S.T., Buske, F.A., Saar, K., Hubner, N., Brandli, A.W. and Schedl, A. (2014) WT1 controls antagonistic FGF and BMP-pSMAD pathways in early renal progenitors. *Nat. Commun.*, **5**, 4444.
20. Kann, M., Ettou, S., Jung, Y.L., Lenz, M.O., Taglienti, M.E., Park, P.J., Schermer, B., Benzing, T. and Kreidberg, J.A. (2015) Genome-wide analysis of Wilms' tumor 1-controlled gene expression in podocytes reveals key regulatory mechanisms. *J. Am. Soc. Nephrol.*, **26**, 2097–2104.
21. Wassarman, P.M. (1987) Early events in mammalian fertilization. *Ann. Rev. Cell Biol.*, **3**, 109–142.
22. Burkart, A.D., Xiong, B., Baibakov, B., Jimenez-Movilla, M. and Dean, J. (2012) Ovastacin, a cortical granule protease, cleaves ZP2 in the zona pellucida to prevent polyspermy. *J. Cell Biol.*, **197**, 37–44.
23. Little, S.E., Hanks, S.P., King-Underwood, L., Jones, C., Rapley, E.A., Rahman, N. and Pritchard-Jones, K. (2004) Frequency and heritability of WT1 mutations in nonsyndromic Wilms' tumor patients: a UK Children's Cancer Study Group Study. *J. Clin. Oncol.*, **22**, 4140–4146.
24. Diller, L., Ghahremani, M., Morgan, J., Grundy, P., Reeves, C., Breslow, N., Green, D., Neuberg, D., Pelletier, J. and Li, F.P. (1998) Constitutional WT1 mutations in Wilms' tumor patients. *J. Clin. Oncol.*, **16**, 3634–3640.
25. Matsushita, K. and Sugiura, Y. (2001) Effect of arginine mutation of alanine-556 on DNA recognition of zinc finger protein Sp1. *Bioorgan. Med. Chem.*, **9**, 2259–2267.
26. Bromberg, Y. and Rost, B. (2007) SNAP: predict effect of non-synonymous polymorphisms on function. *Nucleic Acids Res.*, **35**, 3823–3835.
27. Reddy, J.C., Morris, J.C., Wang, J., English, M.A., Haber, D.A., Shi, Y. and Licht, J.D. (1995) WT1-mediated transcriptional activation is inhibited by dominant negative mutant proteins. *J. Biol. Chem.*, **270**, 10878–10884.
28. Bruening, W., Moffett, P., Chia, S., Heinrich, G. and Pelletier, J. (1996) Identification of nuclear localization signals within the zinc fingers of the WT1 tumor suppressor gene product. *FEBS Lett.*, **393**, 41–47.
29. Chen, L., Mao, S.J., McLean, L.R., Powers, R.W. and Larsen, W.J. (1994) Proteins of the inter-alpha-trypsin inhibitor family stabilize the cumulus extracellular matrix through their direct binding with hyaluronic acid. *J. Biol. Chem.*, **269**, 28282–28287.
30. Ferrer, M., Rodriguez, H., Zara, L., Yu, Y., Xu, W. and Oko, R. (2012) MMP2 and acrosin are major proteinases associated with the inner acrosomal membrane and may cooperate in sperm penetration of the zona pellucida during fertilization. *Cell Tissue Res.*, **349**, 881–895.
31. Staun-Ram, E., Goldman, S., Gabarin, D. and Shalev, E. (2004) Expression and importance of matrix metalloproteinase 2 and 9 (MMP-2 and -9) in human trophoblast invasion. *Reprod. Biol. Endocrinol.*, **2**, 59.
32. Shaw, J.L., Dey, S.K., Critchley, H.O. and Horne, A.W. (2010) Current knowledge of the aetiology of human tubal ectopic pregnancy. *Hum. Reprod. Update*, **16**, 432–444.
33. DeCherney, A.H. and Boyers, S.P. (1985) Isthmic ectopic pregnancy: segmental resection as the treatment of choice. *Fertil. Steril.*, **44**, 307–312.
34. Toska, E. and Roberts, S.G. (2014) Mechanisms of transcriptional regulation by WT1 (Wilms' tumour 1). *Biochem. J.*, **461**, 15–32.

35. Ryan, G., Steele-Perkins, V., Morris, J.F., Rauscher, F.J., 3rd. and Dressler, G.R. (1995) Repression of Pax-2 by WT1 during normal kidney development. *Development*, **121**, 867–875.
36. Klattig, J., Sierig, R., Kruspe, D., Besenbeck, B. and Englert, C. (2007) Wilms' tumor protein Wt1 is an activator of the anti-Mullerian hormone receptor gene Amhr2. *Mol. Cell. Biol.*, **27**, 4355–4364.
37. Sheng, J., Luo, C., Jiang, Y., Hinds, P.W., Xu, Z. and Hu, G.F. (2014) Transcription of angiogenin and ribonuclease 4 is regulated by RNA polymerase III elements and a CCCTC binding factor (CTCF)-dependent intragenic chromatin loop. *J. Biol. Chem.*, **289**, 12520–12534.
38. Lupianez, D.G., Kraft, K., Heinrich, V., Krawitz, P., Brancati, F., Klopocki, E., Horn, D., Kayserili, H., Opitz, J.M., Laxova, R., *et al.* (2015) Disruptions of topological chromatin domains cause pathogenic rewiring of gene-enhancer interactions. *Cell*, **161**, 1012–1025.
39. Winuthayanon, W., Bernhardt, M.L., Padilla-Banks, E., Myers, P.H., Edin, M.L., Hewitt, S.C., Korach, K.S. and Williams, C.J. (2015) Oviductal estrogen receptor alpha signaling prevents protease-mediated embryo death. *eLife*, **4**.
40. Wilhelm, D. and Englert, C. (2002) The Wilms tumor suppressor WT1 regulates early gonad development by activation of Sf1. *Genes Dev.*, **16**, 1839–1851.
41. Gebeshuber, C.A., Kornauth, C., Dong, L., Sierig, R., Seibler, J., Reiss, M., Tauber, S., Bilban, M., Wang, S., Kain, R., *et al.* (2013) Focal segmental glomerulosclerosis is induced by microRNA-193a and its downregulation of WT1. *Nat. Med.*, **19**, 481–487.
42. Seibler, J., Zevnik, B., Kuter-Luks, B., Andreas, S., Kern, H., Hennek, T., Rode, A., Heimann, C., Faust, N., Kauselmann, G., *et al.* (2003) Rapid generation of inducible mouse mutants. *Nucleic Acids Res.*, **31**, e12.
43. Shevchenko, A., Tomas, H., Havlis, J., Olsen, J.V. and Mann, M. (2006) In-gel digestion for mass spectrometric characterization of proteins and proteomes. *Nat. Protoc.*, **1**, 2856–2860.
44. Rappsilber, J., Ishihama, Y. and Mann, M. (2003) Stop and go extraction tips for matrix-assisted laser desorption/ionization, nanoelectrospray, and LC/MS sample pretreatment in proteomics. *Anal. Chem.*, **75**, 663–670.
45. Sambrook, J. and Russell, D.W. (2006) Purification of nucleic acids by extraction with phenol:chloroform. *CSH Protoc.* **2006**.
46. Livak, K.J. and Schmittgen, T.D. (2001) Analysis of relative gene expression data using real-time quantitative PCR and the 2(-Delta Delta C(T)) method. *Methods*, **25**, 402–408.
47. Edgar, R., Domrachev, M. and Lash, A.E. (2002) Gene expression omnibus: NCBI gene expression and hybridization array data repository. *Nucleic Acids Res.*, **30**, 207–210.
48. Vizcaino, J.A., Deutsch, E.W., Wang, R., Csordas, A., Reisinger, F., Rios, D., Dianes, J.A., Sun, Z., Farrah, T., Bandeira, N., *et al.* (2014) ProteomeXchange provides globally coordinated proteomics data submission and dissemination. *Nat. Biotechnol.*, **32**, 223–226.